Comput. Mech. (2006) 38: 323–333
DOI 10.1007/s00466-006-0036-y

ORIGINAL PAPER

Pavel B. Bochev · Clark R. Dohrmann

A computational study of stabilized, low-order C^0 finite element approximations of Darcy equations

Received: 16 October 2005 / Accepted: 23 December 2005 / Published online: 11 February 2006
© Springer-Verlag 2006

Abstract We consider finite element methods for the Darcy equations that are designed to work with standard, low order C^0 finite element spaces. Such spaces remain a popular choice in the engineering practice because they offer the convenience of simple and uniform data structures and reasonable accuracy. A consistently stabilized method [20] and a least-squares formulation [18] are compared with two new stabilized methods. The first one is an extension of a recently proposed polynomial pressure projection stabilization of the Stokes equations [5, 13]. The second one is a weighted average of a mixed and a Galerkin principles for the Darcy problem, and can be viewed as a consistent version of the classical penalty stabilization for the Stokes equations [8]. Our main conclusion is that polynomial pressure projection stabilization is a viable stabilization choice for low order C^0 approximations of the Darcy problem.

Keywords Darcy flow · Mixed Galerkin methods · Stabilization · Projection · Least-squares methods

1 Introduction

Standard C^0 finite element spaces of low polynomial orders remain a popular choice in many engineering applications. Besides their simplicity, they offer reasonable accuracy and uniform data structures when using equal order interpolation. The latter helps to improve parallel efficiency of solution algorithms. However, for many problems of practical interest, C^0 spaces cannot be used without some form of stabilization. In this paper we consider finite element methods for the elliptic boundary value problem

$$\nabla \cdot \mathbf{u} = f \quad \text{in } \Omega, \tag{1}$$

$$\mathbf{u} + \nabla p = 0 \quad \text{in } \Omega, \tag{2}$$

$$\mathbf{u} \cdot \mathbf{n} = 0 \quad \text{on } \Gamma, \tag{3}$$

that are stable and accurate when the velocity $\mathbf{u}$ and the pressure p are approximated by the same, low order C^0 finite element spaces. In (1), (2) and (3), Ω denotes a bounded open region in $\mathbf{R}^n$, $n = 2, 3$ with a Lipschitz continuous boundary Γ and f satisfies the compatibility condition $\int_\Omega f = 0$. Equations (1), (2) and (3) are often called the Darcy flow problem. This model (with appropriate material parameters added) arises in applications from petroleum, civil and electrical engineering such as flow in porous media, heat transfer, and semiconductor device modeling. Similar equations arise in computational algorithms that require projections onto divergence free subspaces. Two examples are fractional step methods [17] for incompressible flow, where the half-step velocity must be projected onto a discretely divergence free manifold, and multiphysics environmental modeling [11] which requires conservative remap of vector fields between different grids.

Elimination of $\mathbf{u}$ from (1), (2) and (3) gives a scalar second order elliptic PDE for the pressure. This problem can be solved by a Galerkin method with C^0 elements. In this case, velocity is a derived quantity whose accuracy is of one order less than the accuracy of the pressure. Thus, when p is the **most** important variable one solves the second order problem, while for applications where $\mathbf{u}$ is more important, one uses the first-order system (1), (2) and (3).

A mixed variational formulation of (1), (2) and (3) is well-posed in $H(\Omega, \text{div}) \times L_0^2(\Omega)$. It is well-known that stable and accurate mixed finite elements for this problem are subject to an inf–sup condition (see [7]). In particular, this condition rules out low-order C^0 approximations of the pressure and velocity. Typically, stable velocity approximations are continuous only in the normal direction and are known as

P.B. Bochev (✉)
Computational Mathematics and Algorithms,
Sandia National Laboratories, P.O. Box 5800,
MS 1110, Albuquerque NM 87185-1110, USA
E-mail: pbboche@sandia.gov
Tel.: +1-505-8441990
Fax: +1-505-8457442

C. R. Dohrmann
Structural Dynamics Research Department,
Sandia National Laboratories, P.O. Box 5800,
MS 0847, Albuquerque, NM, 87185-0847, USA
E-mail: crdohrm@sandia.gov

face elements (see [7]). Mixed methods have valuable properties such as local mass conservation. However, they are more complex to implement and lead to saddle point systems which can be more difficult to solve, unless one is willing to consider hybridization [7]. More importantly, though, lowest order face elements experience problems on non-affine grids where the use of the Piola transform in their definition leads to loss of approximation property. Specifically, on unstructured quadrilateral and hexahedral grids, the lowest order face elements fail to recover constant fields. This leads to a loss of convergence in the velocity variable in the mixed method (see [1, 21]). Therefore, mixed formulations of (1), (2), and (3) that work with standard C^0 element pairs can be very useful on such grids.

Of course, if used with the standard mixed form of (1), (2), and (3), equal-order C^0 finite elements are unstable. To use C^0 elements in the Darcy problem, the mixed weak form must be either modified or replaced by some other form. In this paper we focus on four different possibilities to accomplish this. The first one is to use the classical least-squares approach for the first-order system (1), (2), and (3), formulated in [14, 15, 18]. The second is to stabilize the mixed problem by using the residual of (2). This approach, proposed in [20] is similar to Galerkin least-squares methods for the Stokes equations where stabilization relies on the residual of the momentum equation.

The other two approaches to stabilize (1), (2) and (3) have not been, to the best **of** our knowledge, studied in the literature. The first one extends the polynomial pressure projection stabilization, developed for the Stokes equations in [5, 13], to the mixed variational form of (1), (2) and (3). We note that our method differs from the pressure projection stabilization of Becker and Brack [2] and Codina and Blasco [12] in several important ways. First, both of these methods project the gradient of the pressure variable. In [12] the pressure gradient is projected onto the continuous velocity space which leads to a global problem. In [2] the gradient is projected locally onto element patches by solving small local problems. However, this method requires nested spaces while the method of Codina and Blasco does not need this assumption. In contrast, our approach projects the pressure variable onto a discontinuous polynomial space defined with respect to the original element partition. Consequently, the method is both local and does not require nested grids. A related approach is the pressure jump stabilization method of Silvester [22]. This method is designed for discontinuous pressure spaces and so it cannot be extended to stabilize equal order C^0 formulations. The last method considered in the paper uses a weighted average of the mixed and the Galerkin weak equations. It can be viewed as an extension of the classical penalty stabilization of Brezzi and Pitkaranta [8] obtained by using the weak Galerkin form of the residual. Consequently, this method is consistent.

Since our computational study focuses on methods that rely on standard implementations with low order C^0 elements, we did not include methods that use non-conforming elements [19], edge based assembly [10], or discrete negative norms [6]. For the same reasons we did not consider Discontinuous Galerkin methods. A Discontinuous Galerkin method for the Darcy problem has been recently proposed in [9]. Each one of these methods offers specific advantages and can be used in lieu of mixed methods for (1), (2), and (3). For example, the method of [19] is applicable to the Darcy–Stokes problem, while the DG method in [9] is well-suited for problems with less regular solutions.

The paper is organized as follows. The four methods that are the subject of this study are presented in Sect. 2. Numerical results for the methods are collected in Sect. 3. Our conclusions are summarized in Sect. 4.

2 Stable C^0 finite element formulations

In this paper we consider finite element methods for (1), (2) and (3) that use velocity and pressure approximations of the same interpolation order, and defined with respect to the same partition $\mathcal{T}_h$ of the domain Ω into finite elements Ω_e. For simplicial elements we recall the affine families of Lagrange finite element spaces

$$P_k = \{u^h \in C^0(\Omega) \mid u^h_{|\Omega_e} \in \mathcal{P}_k(\Omega_e);\ \forall \Omega_e \in \mathcal{T}_h\}, \tag{4}$$

where $\mathcal{P}_k(\Omega_e)$ is the space of complete polynomials of degree k defined on the element Ω_e.

For quadrilateral and hexahedral elements we consider the Lagrange spaces

$$Q_k = \{u^h \in C^0(\Omega) \mid u^h_{|\Omega_e} = \hat{u}^h \circ F^{-1};\ \hat{u}^h \in \mathcal{Q}_k(\hat{\Omega}_e)\}, \tag{5}$$

where $\hat{\Omega}_e$ is a reference element, $F : \hat{\Omega}_e \mapsto \Omega_e$ is a bilinear or trilinear mapping, and $\mathcal{Q}_k$ is the space of all polynomials on $\hat{\Omega}_e$ whose degree does not exceed k in each coordinate direction. Unless Ω_e is a parallelogram or a parallelepiped, u^h is not a piecewise polynomial function. We will use the symbol R_k to denote both kinds of finite element spaces. Vector valued finite element spaces will be denoted in bold face, e.g., $\mathbf{R}_k$. We assume that $k = 1$ or $k = 2$.

The spaces R_k have the following approximation property: given a function $u \in H^{k+1}(\Omega)$ there exist $u^h \in R_k$ such that

$$\|u - u^h\|_0 + h\|\nabla u - \nabla u^h\|_0 \le Ch^{k+1}\|u\|_{k+1}. \tag{6}$$

2.1 Polynomial pressure projection stabilization

The mixed form of (1), (2) and (3) is to seek $(\mathbf{u},\ p)$ in $H_0(\Omega, \mathrm{div}) \times L^2_0(\Omega)$ such that

$$\int_\Omega q \nabla \cdot \mathbf{u}\, d\Omega - \int_\Omega f q\, d\Omega = 0 \quad \forall q \in L^2(\Omega), \tag{7}$$

$$\int_\Omega \mathbf{v} \cdot \mathbf{u}\, d\Omega - \int_\Omega p \nabla \cdot \mathbf{v}\, d\Omega = 0 \quad \forall \mathbf{v} \in H_0(\Omega, \mathrm{div}). \tag{8}$$

Equations (7) and (8) are the first-order optimality system for the saddle-point of the Lagrangian

$$L(\mathbf{v}, q) = \frac{1}{2}\int_\Omega |\mathbf{v}|^2 \,\mathrm{d}\Omega - \int_\Omega q(\nabla\cdot\mathbf{v} - f)\,\mathrm{d}\Omega. \tag{9}$$

If we define the bilinear form

$$Q(\mathbf{u}, p; \mathbf{v}, q) = \int_\Omega q\nabla\cdot\mathbf{u}\,\mathrm{d}\Omega + \int_\Omega \mathbf{v}\cdot\mathbf{u}\,\mathrm{d}\Omega - \int_\Omega p\nabla\cdot\mathbf{v}\,\mathrm{d}\Omega, \tag{10}$$

and the linear functional

$$F(\mathbf{v}, q) = \int_\Omega fq\,\mathrm{d}\Omega,$$

problem (7) and (8) can be written compactly as: seek $(\mathbf{u}, p) \in H_0(\Omega, \mathrm{div}) \times L^2_0(\Omega)$ such that

$$Q(\mathbf{u}, p; \mathbf{v}, q) = F(\mathbf{v}, q) \quad \forall(\mathbf{v}, q) \in H_0(\Omega, \mathrm{div}) \times L^2_0(\Omega). \tag{11}$$

To approximate the solution of (7) and (8) we consider the equal-order pair $(\mathbf{V}^h, S^h)$ where

$$\mathbf{V}^h = \mathbf{R}_k \cap H_0(\Omega, \mathrm{div}) \quad \text{and} \quad S^h = R_k \cap L^2_0(\Omega). \tag{12}$$

For $k = 1, 2$ the pair $(\mathbf{V}^h, S^h)$ does not verify the inf–sup condition relevant to (7) and (8). As a result, the discrete mixed weak problem: seek $(\mathbf{u}^h, p^h) \in \mathbf{V}^h \times S^h$ such that

$$\int_\Omega q^h\nabla\cdot\mathbf{u}^h\,\mathrm{d}\Omega - \int_\Omega fq^h\,\mathrm{d}\Omega = 0 \quad \forall q^h \in S^h, \tag{13}$$

$$\int_\Omega \mathbf{v}^h\cdot\mathbf{u}^h - p^h\nabla\cdot\mathbf{v}^h\,\mathrm{d}\Omega = 0 \quad \forall\mathbf{v}^h \in \mathbf{V}^h, \tag{14}$$

is not stable. Following [5, 13], we stabilize (13) and (14) using a local L^2 projection operator onto the discontinuous polynomial space

$$[P_m] = \{q^h \in L^2(\Omega) \mid q^h_{|\Omega_e} \in \mathcal{P}_m(\Omega_e);\ \forall\Omega_e \in \mathcal{T}_h\}, \tag{15}$$

where $m = k-1$. In (15) $\mathcal{T}_h$ can be a simplicial or a non-simplicial partition of Ω into finite elements. Given a function $q \in L^2(\Omega)$ the projection operator $\Pi_m\colon L^2(\Omega) \mapsto [P_m]$ is defined by:

$$\Pi_m p = \arg\min \frac{1}{2}\int_\Omega (\Pi_m q - p)^2\,\mathrm{d}\Omega. \tag{16}$$

Therefore,

$$\Pi_m q = q^h \in [P_m],$$

if and only if

$$\int_\Omega r^h(\Pi_m q - q)\,\mathrm{d}\Omega = 0 \quad \forall r^h \in [P_m]. \tag{17}$$

Equation (17) is a necessary condition for the minimizer in (16). Because $[P_m]$ is discontinuous, (17) uncouples into local element problems

$$\int_{\Omega_e} r^h(\Pi_m q - q)\,\mathrm{d}\Omega_e = 0 \quad \forall r^h \in \mathcal{P}_m(\Omega_e);\ \ \forall\Omega_e \in \mathcal{T}_h, \tag{18}$$

which can be solved independently of each other at the element level. For affine families of piecewise linear elements defined on simplicial triangulations, (18) admits a particularly simple solution. For such elements restrictions of nodal basis shape functions N_i onto an element Ω_e coincide with the barycentrics λ_j, $j = 1, \ldots, n+1$, where n is the space dimension. A simple calculation reveals that

$$\Pi_0\lambda_j = \frac{1}{n+1}. \tag{19}$$

To stabilize the mixed form (10) we consider the projection operator Π_{k-1}, the bilinear form

$$C(p^h, q^h) = \int_\Omega (p^h - \Pi_{k-1}p^h)(q^h - \Pi_{k-1}q^h)\,\mathrm{d}\Omega, \tag{20}$$

and modify (10) to

$$Q_P(\mathbf{u}^h, p^h; \mathbf{v}^h, q^h) = Q(\mathbf{u}^h, p^h; \mathbf{v}^h, q^h) + \alpha C(p^h, q^h), \tag{21}$$

where $\alpha = \hat{\alpha}\frac{1}{L^2}$, $\hat{\alpha}$ is a dimensionless, positive real parameter independent of h, and L is a characteristic length scale. The polynomial pressure projection stabilized method is to seek $(\mathbf{u}^h, p^h)$ in $\mathbf{V}^h \times S^h$, such that

$$Q_P(\mathbf{u}^h, p^h; \mathbf{v}^h, q^h) = F(\mathbf{v}^h, q^h) \quad \forall(\mathbf{v}^h, q^h) \in \mathbf{V}^h \times S^h. \tag{22}$$

This finite element method can also be derived from (9) penalized by

$$\frac{1}{2}C(q, q) = \frac{\alpha}{2}\|(I - \Pi_{k-1})q\|^2_0.$$

Indeed, it is not hard to see that the variational equation in (22) is equivalent to the Euler–Lagrange equation associated with the saddle-point of the *penalized* Lagrangian

$$L_P(\mathbf{v}, q) = \frac{1}{2}\int_\Omega |\mathbf{v}|^2\,\mathrm{d}\Omega - \int_\Omega q(\nabla\cdot\mathbf{v} - f)\,\mathrm{d}\Omega - \frac{\alpha}{2}\|(I - \Pi_{k-1})q\|^2_0. \tag{23}$$

2.2 Galerkin stabilization

Elimination of $\mathbf{u}$ from (1) and (2) gives the second order problem

$$-\triangle p = f \quad \text{in } \Omega, \tag{24}$$

$$\frac{\partial p}{\partial\mathbf{n}} = 0 \quad \text{on } \Gamma, \tag{25}$$

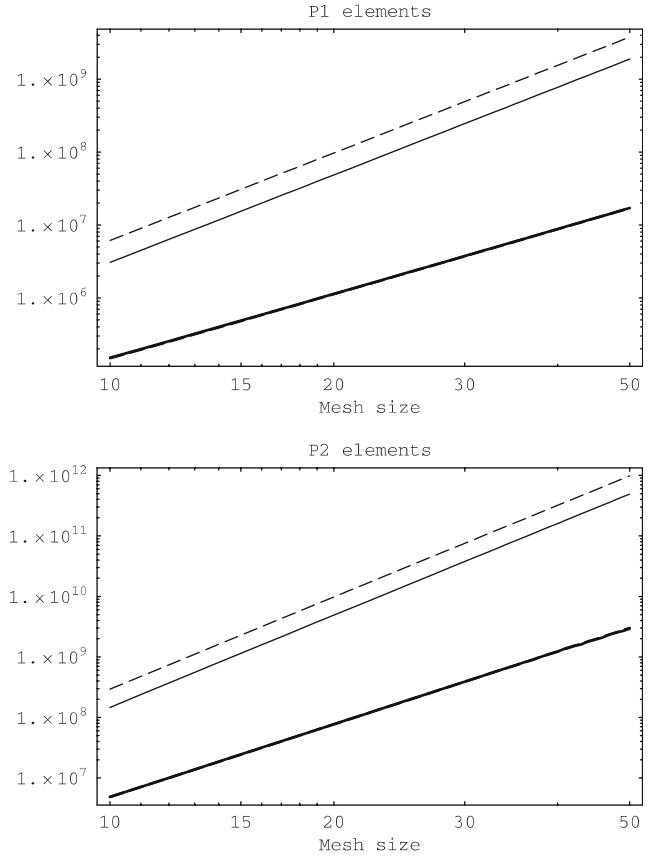

Fig. 1 LAPACK estimates of condition numbers for the four methods

Table 1 Estimated slopes from Fig. 1

	Method			
Elements	PPS	GS	RS	LS
P1	2.91	2.91	3.91	3.90
P2	3.82	3.91	4.91	4.91

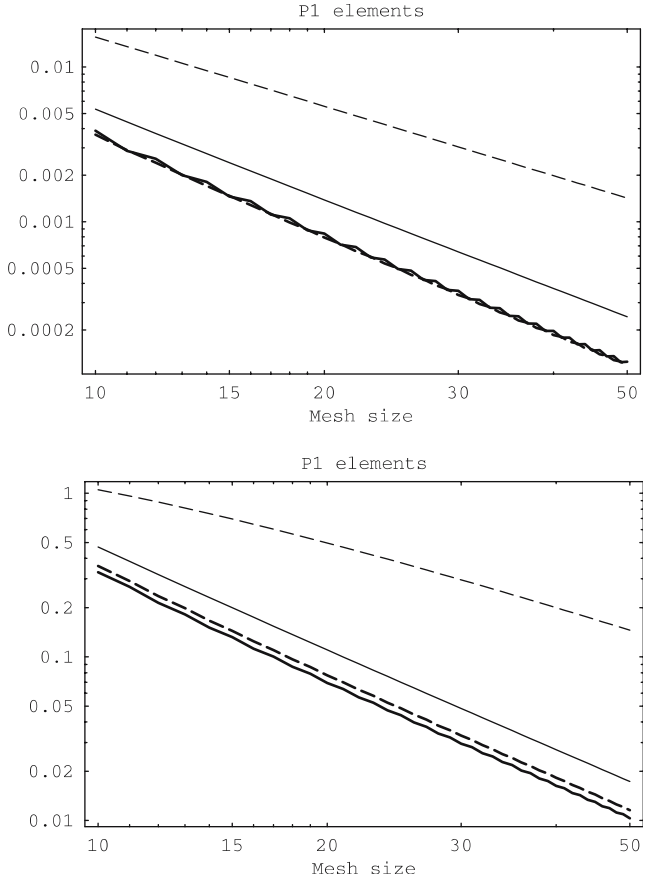

Fig. 2 Velocity L^2 errors for P1 elements. *Top*: Example (39); *bottom*: example (40)

where f is subject to the constraint $\int_\Omega f = 0$. A weak Galerkin form of (24) and (25) is to seek $p \in H^1(\Omega)/\mathbf{R}$ such that

$$G(p, q) = l(q) \quad \forall q \in H^1(\Omega)/\mathbf{R}, \tag{26}$$

where

$$G(p, q) = \int_\Omega \nabla p \cdot \nabla q \, \mathrm{d}\Omega \quad \text{and} \quad l(q) = \int_\Omega f q \, \mathrm{d}\Omega.$$

It is well-known that the Galerkin finite element method: seek $p^h \in S^h/\mathbf{R}$ such that

$$G(p^h, q^h) = l(q^h) \quad \forall q^h \in S^h/\mathbf{R}, \tag{27}$$

is stable and optimally accurate with the C^0 spaces (4) and (5).

To define the second stabilized mixed method for the Darcy problem we modify (10) to

$$Q_G(\mathbf{u}^h, p^h; \mathbf{v}^h, q^h) = Q(\mathbf{u}^h, p^h; \mathbf{v}^h, q^h) + \alpha h^2 G(p^h, q^h), \tag{28}$$

where α is a real, dimensionless parameter independent of h. The *Galerkin* stabilized mixed method is to seek $(\mathbf{u}^h, p^h)$ in $\mathbf{V}^h \times S^h$, such that

$$Q_G(\mathbf{u}^h, p^h; \mathbf{v}^h, q^h) = F_G(\mathbf{v}^h, q^h) \quad \forall (\mathbf{v}^h, q^h) \in \mathbf{V}^h \times S^h, \tag{29}$$

and where

$$F_G(\mathbf{v}^h, q^h) = F(\mathbf{v}^h, q^h) + \alpha h^2 l(q^h).$$

The stabilized method (29) can be viewed as a weighted average of the unstable mixed method (13) and (14) and the stable Galerkin method (27). Alternatively, we can view (29) as obtained by adding the weak residual

$$R(p^h, q^h) = G(p^h, q^h) - l(q^h),$$

weighted by αh^2 to the unstable mixed problem. As a result, the Galerkin stabilized method is consistent in the sense that all sufficiently smooth solutions of the Darcy problem also satisfy (29). Yet another way to derive (29) is to consider the

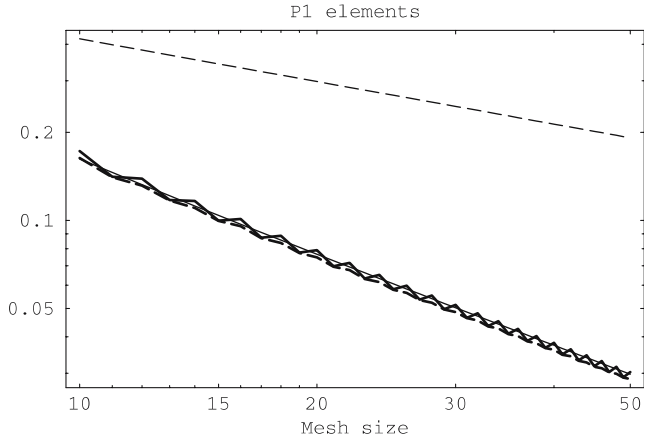

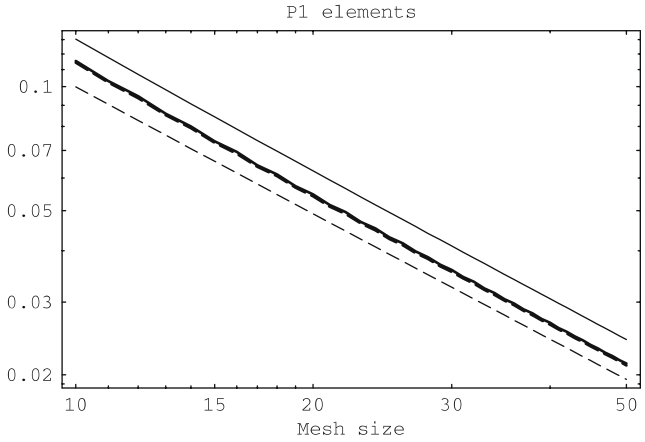

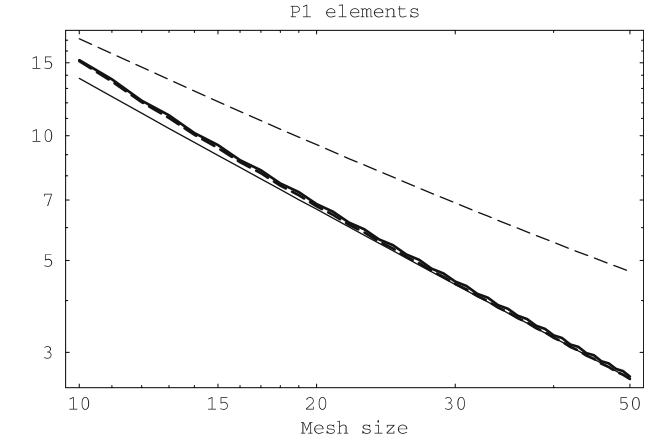

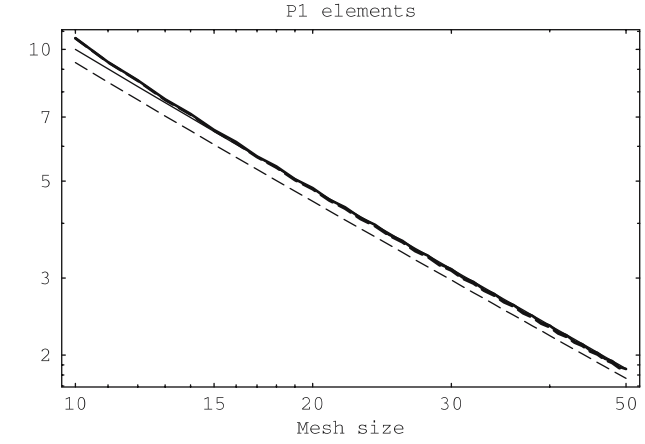

Fig. 3 Velocity H^1 errors for P1 elements. *Top*: Example (39); *bottom*: example (40)

Fig. 4 Velocity $H(\Omega, \mathrm{div})$ errors for P1 elements. *Top*: Example (39); *bottom*: example (40)

Table 2 Estimates of convergence rates for the L^2-norm velocity error

	P1 elements				P2 elements			
Ex.	PPS	GS	RS	LS	PPS	GS	RS	LS
1	2.10	2.11	1.85	1.46	1.96	1.96	1.96	2.00
2	2.00	1.99	1.96	1.38	2.01	2.02	1.89	2.02
BA	2				3			

Table 3 Estimates of convergence rates for the H^1-seminorm velocity error

	P1 elements				P2 elements			
Ex.	PPS	GS	RS	LS	PPS	GS	RS	LS
1	1.01	1.01	1.00	0.47	0.97	0.96	0.96	1.00
2	1.00	1.00	1.00	0.71	1.01	1.02	0.88	1.02
BA	1				2			

Table 4 Estimates of convergence rates for the $H(\Omega, \mathrm{div})$-norm velocity error

	P1 elements				P2 elements			
Ex.	PPS	GS	RS	LS	PPS	GS	RS	LS
1	1.08	1.00	1.00	0.98	0.96	0.96	0.96	2.00
2	1.00	1.00	1.00	0.99	1.01	0.97	0.88	2.00
BA	1				2			

penalized Lagrangian

$$L_G(\mathbf{v}, q) = \frac{1}{2}\int_\Omega |\mathbf{v}|^2 \,\mathrm{d}\Omega - \int_\Omega q(\nabla\cdot\mathbf{v} - f)\,\mathrm{d}\Omega - \alpha h^2\left(\frac{1}{2}\int_\Omega |\nabla q|^2\,\mathrm{d}\Omega - \int_\Omega fq\,\mathrm{d}\Omega\right). \quad (30)$$

We note that the stabilizing term $\alpha h^2 G(p^h, q^h)$ is the same as in the classical *penalty* stabilization of the Stokes equations [8]. However, the presence of the term $\alpha h^2 l(q^h)$ makes (29) a consistent method.

2.3 Strong residual stabilization

An alternative consistently stabilized method was recently proposed in [20]. In this method the mixed form (13) and (14) is stabilized by using the residual of (2). The form (10) is modified to

$$Q_R(\mathbf{u}^h, p^h; \mathbf{v}^h, q^h) = Q(\mathbf{u}^h, p^h; \mathbf{v}^h, q^h) + \frac{1}{2}\int_\Omega (\mathbf{u} + \nabla p)\cdot(-\mathbf{v} + \nabla q)\, \mathrm{d}\Omega. \tag{31}$$

and the stabilized method is to seek $(\mathbf{u}^h, p^h)$ in $\mathbf{V}^h \times S^h$, such that

$$Q_R(\mathbf{u}^h, p^h; \mathbf{v}^h, q^h) = F(\mathbf{v}^h, q^h)\ \forall (\mathbf{v}^h, q^h) \in \mathbf{V}^h \times S^h. \tag{32}$$

It is straightforward to check that

$$Q_R(\mathbf{v}^h, q^h; \mathbf{v}^h, q^h) = \frac{1}{2}\left(\|\mathbf{v}^h\|_0^2 + \|\nabla q\|_0^2\right),$$

that is $Q_R(\cdot,\cdot)$ is coercive in $\mathbf{L}^2(\Omega) \times H^1(\Omega)/\mathbf{R}$. In [20] the following error estimate is proved for the finite element solutions of (32):

$$\|\mathbf{u} - \mathbf{u}^h\|_0 + \|p - p^h\|_1 \le \left(\inf_{\mathbf{v}^h \in \mathbf{V}^h} \|\mathbf{u} - \mathbf{v}^h\|_0 + \inf_{q^h \in S^h} \|p - q^h\|_1\right). \tag{33}$$

The finite element method (32) can be derived from (9) penalized by the least-squares term

$$\frac{1}{4}\|\mathbf{v} + \nabla q\|_0^2.$$

Indeed, it is easy to check that (32) is the Euler–Lagrange equation for the *penalized* Lagrangian

$$L_R(\mathbf{v}, q) = \frac{1}{2}\int_\Omega |\mathbf{v}|^2\, \mathrm{d}\Omega - \int_\Omega q(\nabla\cdot\mathbf{v} - f)\, \mathrm{d}\Omega - \frac{1}{4}\|\mathbf{v} + \nabla q\|_0^2. \tag{34}$$

We remark that in many cases stabilized methods can be derived through an enrichment of a Galerkin method by bubble functions followed by static condensation [16]. The pressure-projection method (22), on the other hand, is an exception to this rule. Its structure resembles that of a penalty method with the crucial difference that the stabilizing form (20) is symmetric and semi-definite rather than positive definite, as in penalty methods. Therefore, the role of the stabilizing term is to act as a filter that removes destabilizing modes.

2.4 A Least-squares method

The polynomial pressure projection method (22), the Galerkin stabilized method (29) and the residual stabilized method (32) are derived from the unstable mixed form (10), i.e., they represent regularizations of the same mixed variational equation. A least-squares method, on the other hand, is based on a completely new variational principle associated with unconstrained global minimization of a problem-dependent quadratic functional. For a survey of least-squares methods we refer to [3].

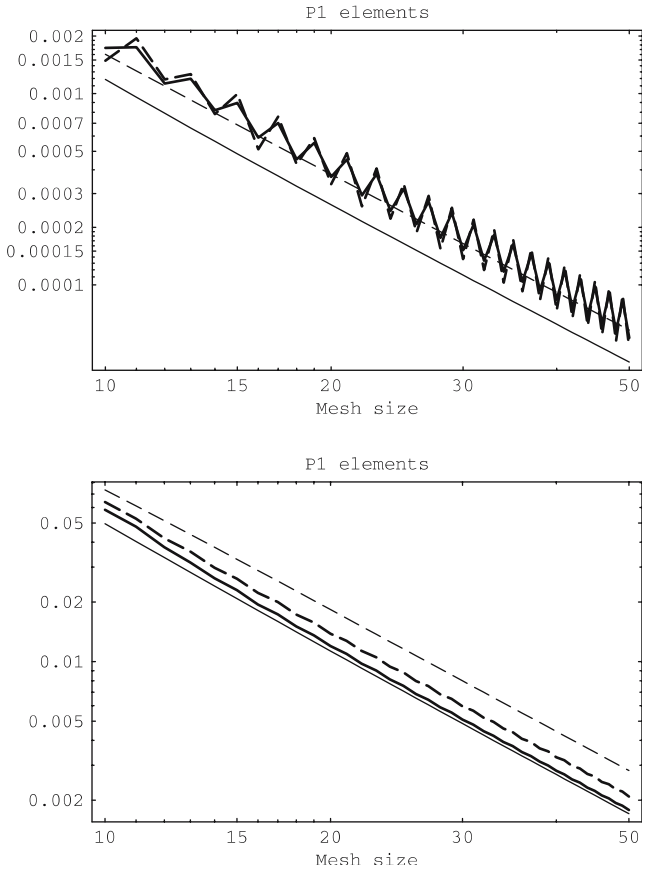

Fig. 5 Pressure L^2 errors for P1 elements. *Top*: Example (39); *bottom*: example (40)

In this paper we compare (22), (29) and (32) with a method based on minimization of the functional

$$J(\mathbf{v}, q) = \frac{1}{2}\left(\|\nabla\cdot\mathbf{v} - f\|_0^2 + \|\mathbf{v} + \nabla q\|_0^2\right). \tag{35}$$

This functional, defined by summing up the L^2 norms of the residuals of (1) and (2), was originally proposed in [18]. Least-squares methods for (1) and (2) that use negative norms were developed by Bramble et al. [6]. Such methods require approximation of the inner product on H^{-1} and for this reason they are not included in our study.

It is easy to see that all sufficiently smooth solutions of (1) and (2) are minimizers of (35) and vice versa. This observation is the basis of least-squares finite element methods for the Darcy flow: such methods are defined by restricting minimization of (35) to the finite element pair $(\mathbf{V}^h, S^h)$. The minimizers can be computed by setting the first variations of the least-squares functional to zero, i.e., by solving the Euler–Lagrange equation: seek $(\mathbf{u}^h, p^h) \in \mathbf{V}^h \times S^h$ such that

$$Q_{\mathrm{LS}}(\mathbf{u}^h, p^h; \mathbf{v}^h, q^h) = F_{\mathrm{LS}}(\mathbf{v}^h, q^h) \quad \forall (\mathbf{v}^h, q^h) \in \mathbf{V}^h \times S^h, \tag{36}$$

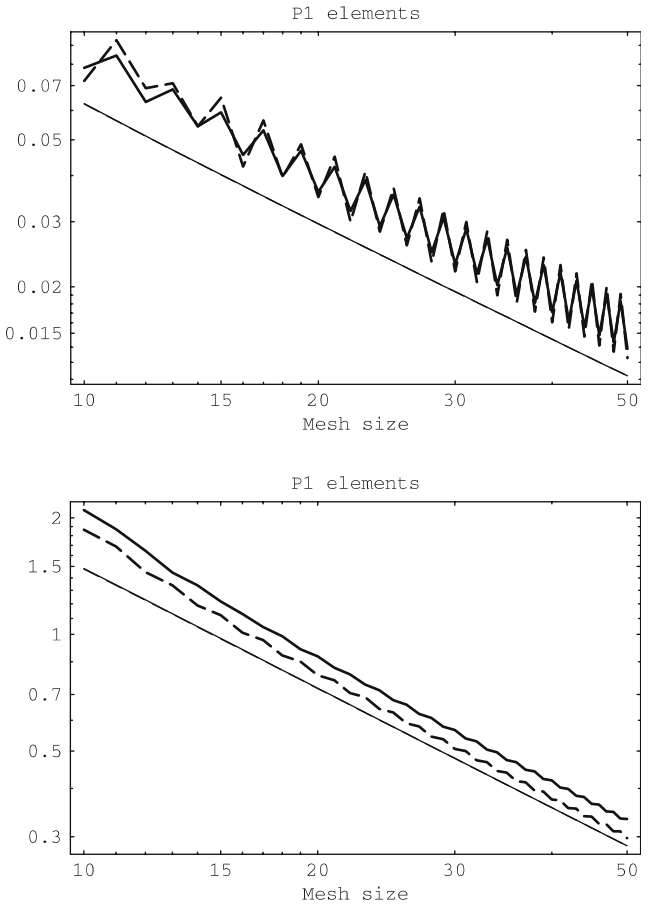

Fig. 6 Pressure H^1 errors for P1 elements. *Top*: Example (39); *bottom*: example (40)

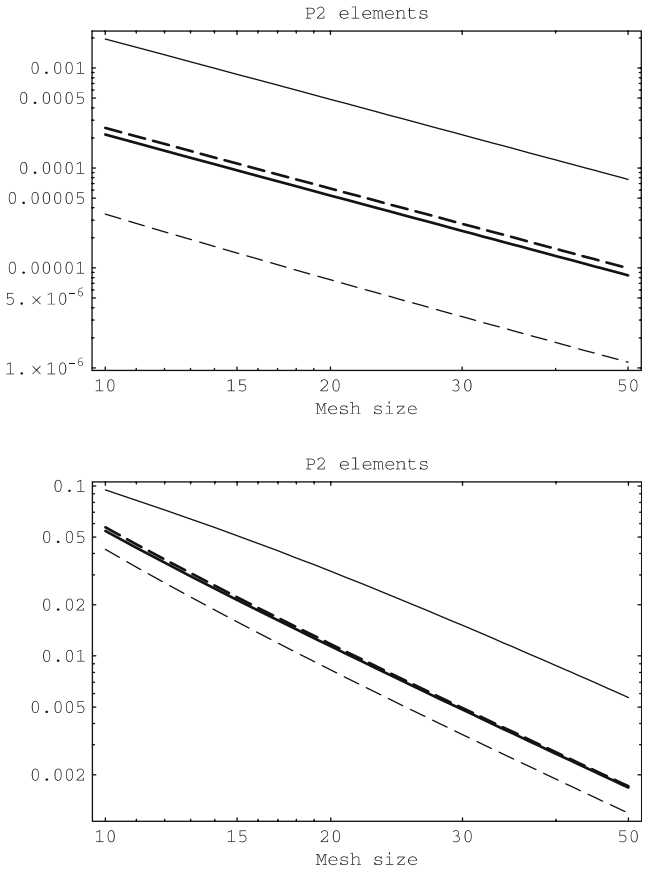

Fig. 7 Velocity L^2 errors for P2 elements. *Top*: Example (39); *bottom*: example (40)

where

$$Q_{\mathrm{LS}}(\mathbf{u}^h, p^h; \mathbf{v}^h, q^h) = \int_\Omega \nabla\cdot\mathbf{u}^h\,\nabla\cdot\mathbf{v}^h\,\mathrm{d}\Omega + \int_\Omega \left(\mathbf{u}^h+\nabla p^h\right) \times \left(\mathbf{v}^h+\nabla q^h\right)\mathrm{d}\Omega,$$

and

$$F_{\mathrm{LS}}(\mathbf{v}^h, q^h) = \int_\Omega f\nabla\cdot\mathbf{v}^h\,\mathrm{d}\Omega.$$

The least-squares method is consistent because all sufficiently smooth solutions of the Darcy problem satisfy the weak equation (36). The least-squares form is coercive on $H(\Omega,\mathrm{div})\times H^1(\Omega)$, that is,

$$Q_{\mathrm{LS}}(\mathbf{u}, p; \mathbf{u}, p) \geq C\left(\|\mathbf{u}\|^2_{H(\Omega,\mathrm{div})} + \|p\|_1^2\right), \tag{37}$$

for all $(\mathbf{u}, p)\in H(\Omega,\mathrm{div})\times H^1(\Omega)$. The form is also continuous and, using standard elliptic finite element arguments, one can show that

$$\|\mathbf{u}-\mathbf{u}^h\|_{H(\Omega,\mathrm{div})} + \|p-p^h\|_1 \leq C\left(\inf_{\mathbf{v}^h\in\mathbf{V}^h}\|\mathbf{u}-\mathbf{v}^h\|_{H(\Omega,\mathrm{div})} + \inf_{q^h\in S^h}\|p-q^h\|_1\right). \tag{38}$$

For further details we refer to [15, 14, 18].

3 Numerical study

The main goal of our study is to compare and contrast the accuracy of the four finite element methods for (1) and (2) that work with the equal order finite element pair (12). We take Ω to be the unit square and $\mathcal{T}_h$ to be a uniform partition of Ω into triangles. Therefore, (12) consists of C^0 piecewise linear or quadratic elements on triangles.

To asses numerical convergence rates, an exact analytic solution is selected and then inserted into the first-order system (1) and (2) to obtain a right hand side and a boundary function that match this solution. Our first example has an exact pressure solution

$$p = \sin\, y\cos\, x + xy^2 - \frac{1}{6} - (\sin\, 1)(1-\cos\, 1). \tag{39}$$

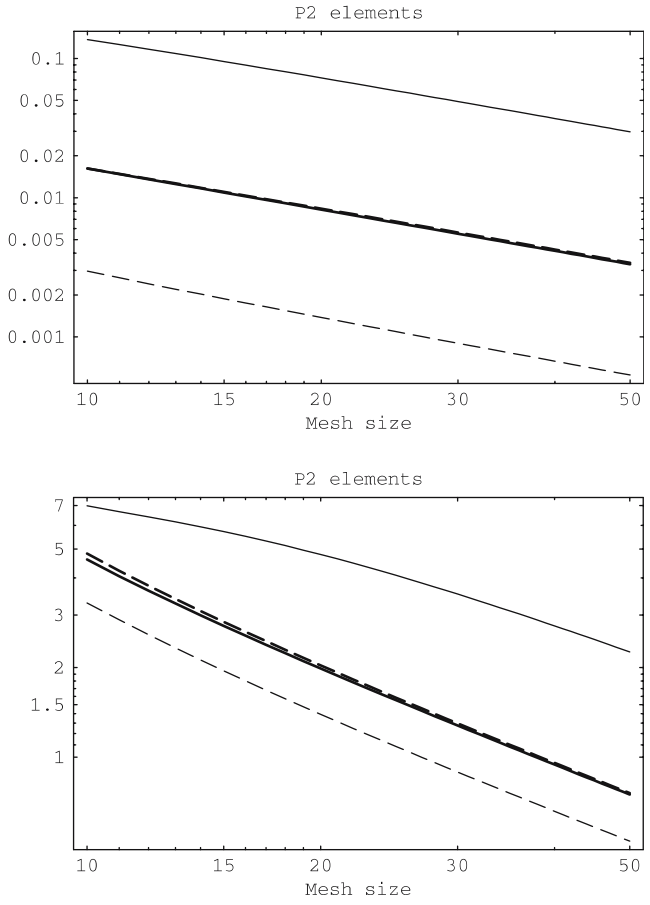

Fig. 8 Velocity H^1 errors for P2 elements. *Top*: Example (39); *bottom*: example (40)

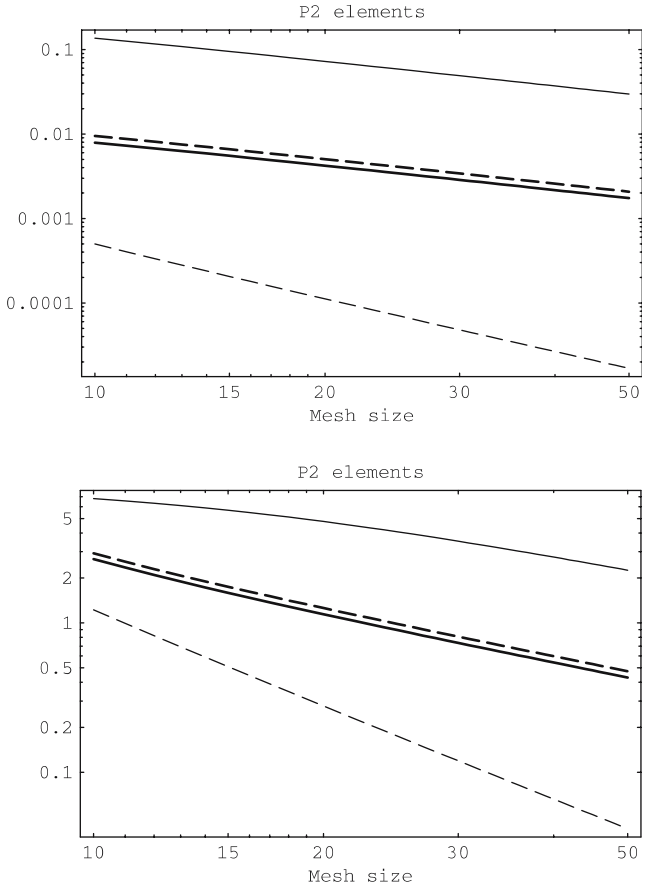

Fig. 9 Velocity $H(\Omega, \mathrm{div})$ errors for P2 elements. *Top*: Example (39); *bottom*: example (40)

The exact velocity is defined by (2), that is, $\mathbf{u} = -\nabla p$. The normal component of the velocity is not zero on the boundary and is approximated by its nodal boundary interpolant.

The second example uses an exact solution from [20] in which the pressure is given by

$$p = \sin\, 2\pi x \cos\, 2\pi y \tag{40}$$

The exact velocity is determined from (2) and the inhomogeneous boundary data is treated in the same way as in the first example. Note that in both examples the pressure has zero mean as required for solvability.

To estimate the convergence rates we solved the two test examples using the four stabilized methods on a sequence of uniform triangulations $\mathcal{T}_h$ with P_1 and P_2 finite element spaces. The first and the last triangulation in the sequence have 162 and 4,802 elements, respectively. The number of variables for P_1 elements on the first and last grids is 260 and 7,300 respectively; for P_2 elements variables increase from 1,007 to 29,007. All algebraic systems are solved using direct solvers from LAPACK. This is done to reduce the possibility of numerical pollution in the errors from insufficiently converged iterative solutions. Then, we compute a least-squares straight line fit to the error data and take the negative slope of this line as an estimate of the convergence rate.

In all plots results by the different methods are marked as follows:

- solid thick line: method (22);
- dashed thick line: method (29);
- solid thin line: method (32);
- dashed thin line: method (36).

Let $(\mathbf{u}^h_{\mathrm{RS}}, p^h_{\mathrm{RS}})$ and $(\mathbf{u}^h_{\mathrm{LS}}, p^h_{\mathrm{LS}})$ denote the finite element solutions of the residual stabilized mixed method (32), and the least-squares method (36), respectively. From [20] and [18] we know that

$$\|\mathbf{u} - \mathbf{u}^h_{\mathrm{RS}}\|_0 + \|p - p^h_{\mathrm{RS}}\|_1 = O(h^k), \tag{41}$$

and

$$\|\mathbf{u} - \mathbf{u}^h_{\mathrm{LS}}\|_{H(\Omega,\mathrm{div})} + \|p - p^h_{\mathrm{LS}}\|_1 = O(h^k), \tag{42}$$

where $k = 1$ for P_1 elements and $k = 2$ for P_2 elements. Error estimates for (22) and (29) are unavailable, and so by our numerical study we seek to gain some insight into their performance. In the experiments we used (22) with $\alpha = 0.5$ for Example (39), and $\alpha = 10$ for Example (40) in order to make the error values of all methods comparable with each other and easy to plot on the same graph. In practice, a single value of α, say $\alpha = 1$, can be used in all circumstances.

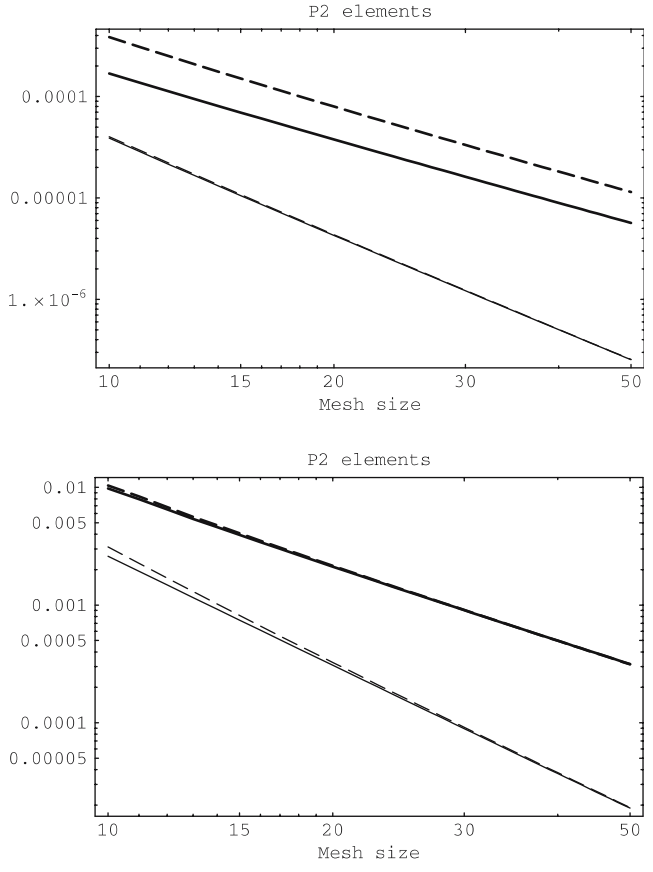

Fig. 10 Pressure L^2 errors for P2 elements. *Top*: Example (39); *bottom*: example (40)

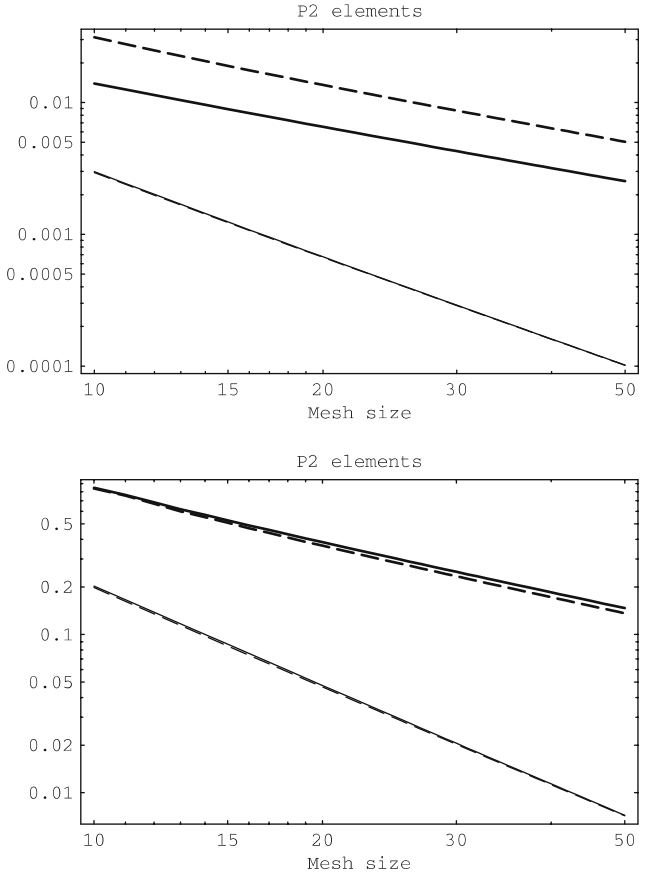

Fig. 11 Pressure H^1 errors for P2 elements. *Top*: Example (39); *bottom*: example (40)

The Galerkin stabilized method (29) also requires selection of a weight. However, being a weighted average of two different weak equations, it tends to be more sensitive to the choice of α, unless the grid is sufficiently fine. If α is very large, (29) is dominated by the primal Galerkin formulation and velocity approximations degrade. In the experiments we used the values $\alpha = 0.01$ and $\alpha = 1$ for the first and the second example, respectively.

We start by inspecting condition number estimates for each method, obtained by using LAPACK routines. This data is summarized in Fig.1 and Table 1. The least-squares method leads to matrices with the highest condition numbers, followed by the residual stabilized method, and the two new methods. The lines for the pressure projection and the Galerkin stabilized methods overlap, meaning that their matrices have essentially the same condition numbers. The data in Table 1 shows that least-squares and residual stabilization have condition numbers with the same asymptotic order. The asymptotic order of the pressure projection condition numbers equals that of the Galerkin stabilized method and is one order of magnitude less than condition numbers of the other two methods.

Next we consider convergence of finite element solutions. We report $L^2(\Omega)$, $H(\Omega, \mathrm{div})$ and H^1-seminorm velocity errors and $L^2(\Omega)$ and $H^1(\Omega)$-seminorm pressure errors. The last row in the tables **with** convergence rate estimates lists the best approximation error (6) for P_1 and P_2 elements.

Results for P_1 elements are discussed next. Figures 2, 3 and 4 show velocity errors for the two example problems. The $H(\Omega, \mathrm{div})$ errors for all four methods are very close, especially for the second example problem. We note that $H(\Omega, \mathrm{div})$ asymptotic errors are asserted only for the least-squares method. The L^2 and H^1-seminorm errors in the velocity are fairly close for (22), (29) and (32), while the least-squares solution clearly lags behind. These observations are quantified by the data in Tables 2, 3, and 4 which suggest optimal, first-order convergence in $H(\Omega, \mathrm{div})$ for all four methods, and suboptimal (by approximately half an order) convergence of the $L^2(\Omega)$ velocity error in the least-squares method. This confirms earlier studies in [15] that show suboptimal L^2 velocity convergence unless $\mathcal{T}_h$ has the Grid Decomposition Property, or is approximated by BDM elements (see [4]).

Somewhat surprisingly, we see that the inconsistent pressure projection stabilized method has the same order of convergence as the consistently stabilized methods (29) and (32). This is despite the fact that for P_1 elements, the pressure projection stabilization term (20) is formally of first order.

The pressure variable appears to be approximated equally well by all four finite element methods. This can be seen by

Table 5 Estimates of convergence rates for the L^2-norm pressure error

	P1 elements				P2 elements			
Ex.	PPS	GS	RS	LS	PPS	GS	RS	LS
1	2.02	2.00	2.00	1.99	2.00	2.03	2.99	3.00
2	2.00	2.00	2.00	2.00	2.00	2.02	2.97	3.00
BA	2				3			

Table 6 Estimates of convergence rates for the H^1-seminorm pressure error

	P1 elements				P2 elements			
Ex.	PPS	GS	RS	LS	PPS	GS	RS	LS
1	1.01	0.97	1.00	1.00	1.00	1.03	2.00	2.00
2	1.00	1.01	1.00	1.00	1.01	1.02	2.00	2.00
BA	1				2			

the error plots in Figs. 5 and 6, and the data in Tables 5 and 6. An interesting feature of the pressure projection and Galerkin stabilized methods is the alternating behavior of some errors for odd and even numbered meshes. This feature is more pronounced for the pressure errors in the first example problem. The important observation is that convergence rates on odd and even numbered grids are identical, which means that the alternating behavior does not affect the asymptotic convergence of the pressure. This aspect of the method together with its better than expected convergence rates calls for further theoretical investigation.

We now turn attention to P_2 elements. Figures 7, 8, and 9 and Tables 2, 3 and 4 show velocity errors and convergence rate estimates for the two example problems. Looking at L^2 and H^1 velocity errors we see that all four methods converge at about the same rate. However, these rates are one order less than the best approximation error for P_2 elements, i.e., the four methods have suboptimal convergence rates with respect to these norms. This is not so for the $H(\Omega, \mathrm{div})$ error. Here, the least-squares method exhibits the optimal rate of $O(h^2)$ and clearly outperforms all other schemes which are only first-order accurate. This behavior is consistent with (41) and (42), since least-squares is the only formulation that is provably stable in $H(\Omega, \mathrm{div})$.

According to (42) and (41) least-squares and residual stabilized methods should yield optimal pressure convergence in $H^1(\Omega)$. Figures 10 and 11 and Tables 5 and 6 confirm this. While not implied by (42) and (41), the $L^2(\Omega)$-norm convergence of the pressure is also optimal. The pressure-projection method is not consistent and for P_2 elements the stabilizing term (20) is second order accurate. While for P_1 elements the method converged better than expected, Tables 5 and 6 show that this is not the case for P_2 elements. Note that the Galerkin stabilized method exhibits the same rates.

4 Conclusions

We presented a computational study of four finite element methods for the Darcy problem that are stable when the same low order C^0 finite element spaces are used to approximate velocity and pressure variables. The first three of the studied methods are based on regularization of the mixed variational form of the Darcy problem and two of them appear to be new. We showed how these methods can be obtained by regularization of the associated Lagrangian saddle-point functional. The fourth method was a least-squares formulation obtained by minimization of a problem-dependent energy functional.

Our study reveals that polynomial pressure projection and Galerkin-stabilized mixed methods have similar performance. For P_1 elements their accuracy is competitive with that of least-squares and Galerkin least squares methods, while their matrix condition numbers are better. Between the two methods we give a preference to the polynomial pressure projection algorithm because it is less sensitive to the choice of a dimensionless parameter. Another important argument in favor of the pressure projection approach is that it can be used to stabilize the incompressible Stokes equations [5, 13]. This opens up a possibility to use one simple procedure to stabilize both the Darcy and Stokes equations, as well as the combination Darcy–Stokes problem. Neither the least-squares nor the Galerkin least-squares methods considered in this paper can be used in this context. Thus, we can conclude that for low order C^0 elements, pressure projection stabilization is a viable alternative to the existing approaches.

Acknowledgements Sandia is a multiprogram laboratory operated by Sandia Corporation, a Lockheed-Martin Company, for the United States Department of Energy's National Nuclear Security Administration under contract DE-AC-94AL85000.

References

1. Arnold D, Boffi D, Falk R (2002) Approximation by quadrilateral finite elements. Math Comput 71:909–922
2. Becker R, Braack M (2001) A finite element pressure gradient stabilization for the Stokes equations based on local projections. Calcolo 38:173–199
3. Bochev P, Gunzburger M (1998) Least-squares finite element methods for elliptic equations. SIAM Rev 40(4):789–837
4. Bochev P, Gunzburger M (2005) On least-squares finite element methods for the Poisson equation and their connection to the Dirichlet and Kelvin principles. SIAM J Num Anal 43(1):340–362
5. Bochev P, Dohrmann C, Gunzburger MD (2005) Stabilization of low-order mixed finite elements for the Stokes equations. SIAM J Num Anal (To appear)
6. Bramble J, Lazarov R, Pasciak J (1994) A least squares approach based on a discrete minus one inner product for first order systems. Technical report 94-32, Mathematical Science Institute, Cornell University
7. Brezzi F, Fortin M (1991) Mixed and hybrid finite element methods. Springer Berlin Heidelberg, New York
8. Brezzi F, Pitkaranta J (1984) On stabilization of finite element approximations of the Stokes equations. In: Hackbusch W (ed) Efficient solution of elliptic systems. Vieweg, Wiesbaden
9. Brezzi F, Hughes TJR, Marini LD, Masud A (2005) Mixed discontinuous Galerkin methods for Darcy flow. J Sci Comput 22(23):119–145
10. Burman E, Hansbo P (2002) A unified stabilized method for Stokes and Darcy's equations. Chalmers finite element center preprint 2002–2015, Chalmers University of Technology, Goteberg
11. Carey GF, Bicken G, Carey V, Berger C, Sanchez J (2001) Locally constrained projections. Int J Numer Methods Eng 50:549–577

12. Codina R, Blasco J (1997) A finite element formulation for the Stokes problem allowing equal order velocity-pressure interpolation. Comput Methods Appl Mech Eng 143:373–391
13. Dohrmann C, Bochev P (2004) A stabilized finite element method for the Stokes problem based on polynomial pressure projections. Int J Numer Methods Fluids 46:183–201
14. Fix G, Gunzburger M (1978) On least squares approximations to indefinite problems of the mixed type. Int J Numer Methods Eng 12:453–469
15. Fix G, Gunzburger M, Nicolaides R (1979) On finite element methods of the least-squares type. Comput Math Appl 5:87–98
16. Franca L, Russo A (1996) Deriving upwinding, mass lumping and selective reduced integration by residual free bubbles. Appl Math Lett 9:83–88
17. Guermond J.L, Quartapelle L (1998) On the approximation of the unsteady Navier-Stokes equations by finite element projection methods. Num Math 80:207–238
18. Jesperson D (1977) A least-squares decomposition method for solving elliptic equations. Math Comput 31:873–880
19. Mardal K, Tai XC, Winther R (2002) A robust finite element method for Darcy–Stokes flow. SIAM J Numer Anal 40(5):1605–1631
20. Masud A, Hughes TJR (2002) A stabilized finite element method for Darcy flow. Comput Methods Appl Mech Eng 191:4341–4370
21. Russel T, Naff RL, Wilson JD (2002) Shape functions for three-dimensional control-volume mixed finite-element methods on irregular grids. In: Hassanizadeh SM et al (eds) Computational methods in water resources, vol 1. Elsevier, Amsterdam, pp 359–366
22. Silvester DJ (1994) Optimal low order finite element methods for incompressible flow. Comput Methods Appl Mech Eng 111:357–368